Desalination and Water Treatment
www.deswater.com
doi: 10.5004/dwt.2022.28072

248 (2022) 149–162
February

Preparation and application of polyethersulfone ultrafiltration membrane incorporating NaX zeolite for lead ions removal from aqueous solutions

Haider N. Alfalahy, Sama M. Al-Jubouri*

Department of Chemical Engineering, College of Engineering, University of Baghdad, Aljadria, Baghdad, Postcode: 10071, Iraq, emails: sama.al-jubouri@coeng.uobaghdad.edu.iq (S.M. Al-Jubouri), ORCID (0000-0001-5080-411X), h.abdul-ameer1207@coeng.uobaghdad.edu.iq (H.N. Alfalahy)

Received 17 August 2021; Accepted 25 December 2021

ABSTRACT

Polyethersulfone (PES) ultrafiltration membrane incorporating NaX zeolite crystals as an ion exchange material was prepared and examined for lead ions (Pb(II)) removal from aqueous solutions. A powder NaX zeolite was synthesized by a hydrothermal technique and characterized using X-ray diffraction (XRD), scanning electron microscope (SEM), energy-dispersive analysis by X-ray (EDAX), and Fourier transforms infrared spectroscopy (FTIR). Then, it was ground and added to a casting solution of 20%wt. PES in dimethylformamide (DMF). Mixed matrix membranes (MMM's) of NaX zeolite/PES were fabricated using the phase inversion method. The prepared membranes were characterized in terms of permeability, contact angle, porosity, thickness, and surface morphology using SEM, Atomic force microscopy (AFM), EDAX, and FTIR. The effect of initial metal solution pH (2–7), initial metal ion concentration (50–200 ppm), and initial feed temperature (25°C, 36°C, and 46°C) on the treatment efficiency and permeate flux was investigated at transmembrane pressure (TMP) of 1.6 bar. The results showed that the permeation flux of the prepared membranes was higher than the base membrane due to enhancing the membrane's properties such as hydrophilicity by adding NaX zeolite. The highest removal percentage of Pb(II) ions (97%) was obtained at pH solution of 6, temperature solution of 25°C, TMP of 1.6 bar, and initial Pb(II) ions concentration of 50 ppm using M3. It was found that M3 has a much higher adsorption capacity than the other prepared membranes.

Keywords: Mixed matrix membranes; NaX zeolite; Lead ions; Ultrafiltration; Ion exchange; Adsorption capacity

1. Introduction

Heavy metals are released into the environment due to human activities and natural phenomena [1]. Municipal and industrial wastewaters, that are released from mining operations, metal plating facilities, electroplating, battery manufacture, electronic device manufactures, fertilizer, chemical pharmaceutical, dyestuffs, and other industries, are mostly the potential sources of heavy metal ions [2,3]. Heavy metals have lethal and toxic effects on the public health and environment when their concentrations exceed the allowable levels in the discharges to the water sink [4,5]. The dangers of the presence of heavy metal ions in the water even at very low concentrations arise from their characteristics. Heavy metals are highly soluble, non-biodegradable, able to transfer to the human and animal bodies through food chains which cause various diseases and disorders [6,7].

* Corresponding author.

Lead is a highly toxic heavy metal and it is dangerous to human health because it causes anemia, permanent brain damage, kidney dysfunction, and different symptoms related to the nervous system [8] Therefore, the world health organization limits the concentration of lead in water to just below 0.01 mg/L [9]. Treatment of industrial wastewaters from toxic metals before discharging into ecosystems does not find appropriate attention in developing countries despite these contaminants' hazards. In recent years, many efforts have been made to remove toxic metals from industrial wastewater due to new regulations imposed regarding environmental protection [10]. Different treatment methods have been studied to remove heavy metal ions such as coagulation–precipitation, flotation, flocculation, electroflotation, solvent, evaporation, extraction, membrane separation, ion exchange and adsorption [11–13]. Some of these methods are cost-effective and efficient for the processes encompassing low concentrations of pollutants such as adsorption [14,15] and ion exchange [16,17]. However, the most obvious drawbacks accompanied with applying the others are that low capacity, deficiency of selectivity, high initial installation cost, operation or regeneration difficulty, problems of slag disposal and extra chemical injection [18,19]. Membrane processes including reverse osmosis (RO), nanofiltration (NF), ultrafiltration (UF) and microfiltration (MF) have appeared as potential treatment processes and have been considered promising technologies for removing pollutants from water [18,20].

Applying the membrane techniques for the environmental protection sector provides several advantages such as eliminating the necessity of adding chemical materials, reducing the energy consumption, continuous separation mode, separation at moderate environment conditions, working in hybrid processes (easily connected to other unit processes) and working as a modular system (possibility of increasing the capacity) [21]. The water production rate and heavy metal removal efficiency depend on some main factors that significantly influence the overall performance of membranes. These features determine the potential application of membranes in aqueous media such as surface charge, pore size, pore size distribution, degree of membrane hydrophilicity, presence of functional groups that assist the separation process and solution flow [22].

Polyethersulfone (PES) membrane is one of the most common ultrafiltration membranes used in water treatment, can remove prevalent and harmful water components, such as viruses, proteins, pathogens, and colloids but it is less able to remove heavy metal ions [23]. When inorganic additives such as zeolite, Fe–Mn binary oxide (FMBO), metal organic framework (MOF), and graphene oxide (GO) are incorporated into the polymeric matrix, a new type of membrane named mixed matrix membranes (MMM's) is formed. MMM's have a high ability to heavy metals removal because of the beneficial property of the synergistic effects offered by the inorganic particles, highly selective and high surface area [24,25]. A significant benefit in the usage of zeolite as an ion-exchange material because zeolite contains cations (sodium, potassium, or calcium). These cations are exchangeable with other positive cations in solutions such as lead, cadmium, zinc, and manganese [26]. Zeolites are known as important microporous materials composed of $[SiO_4]^{4-}$ and $[AlO_4]^{5-}$ tetrahedra to form an open system of channels and pores. This porous system contains easily exchangeable cations and zeolitic water which is important to conduct the separation process by adsorption or ion exchange and different catalysis processes [27,28]. In addition, zeolite has a hydrophilic property that enhances the permeation flux of MMM's.

In this study, PES membranes were modified by incorporating NaX zeolite to form an effective MMM. The performance of the prepared membranes will be examined at different initial metal ions concentrations, solution pH and temperature.

2. Experimental

2.1. Materials

The commercial PES polymer with a molecular weight of 58,000 g/mol as a membrane material supplied by Ultrason E 6020P and dimethylformamide (DMF) with a molecular weight of 73.10 g/mol as an organic solvent supplied by scharlab (Spain/European Union) were used for the preparation of the PES UF membranes. Sodium silicate (32–33%wt. SiO_2) purchased from Lab. UAE Company, sodium aluminate (55–56%wt. Al_2O_3) supplied by RiedeldeHaen and sodium hydroxide (97%wt.) supplied by Fisher scientific were used for preparing NaX zeolite. Lead nitrate (99%wt.) supplied by Thomas Baker was utilized to prepare metal aqueous solutions. Hydrochloric acid (36%) supplied by the BDH laboratory was used to study the effect of pH of metal ions solutions.

2.2. Synthesis of NaX zeolite

NaX zeolite was prepared via the hydrothermal method, according to the method presented by [29,30], in which, aluminosilicate gel was made by mixing sodium aluminate with sodium silicate in an alkaline medium solution made of NaOH. The zeolite formula chosen to obtain amorphous aluminosilicate gel was: 3.9 Na_2O:Al_2O_3:3 SiO_2:156 H_2O [29]. The prepared aluminosilicate gel was continually stirred at room temperature for 24 h. Then, the reaction gel was put in a sealed crystallization reactor and heated at 100°C for 6 h in an oven. The product was washed with de-ionized water until the pH value reached just above 8 and overnight dried at 70°C. The resultant powder zeolite was then ground by a ball mill to have it in the nanoscale.

2.3. Preparation of PES ultrafiltration membrane

PES-based membrane (M0) was prepared by the phase inversion method per the steps mentioned in [31]. 20%wt. PES polymer was dissolved in 80%wt. of DMF with continuous stirring at 200 rpm until the solution became homogeneous. The solution was then left for a while to allow the complete release of air bubbles. After that, the solution was cast on a clean glass plate using a casting knife. The glass plate was immediately immersed in a coagulation bath of water at 25°C. The formed membranes were stored in deionized water for 4 d for complete removal of the

residual solvent. Then the PES membranes were dried at room temperature for about 24 h.

2.4. Preparation of zeolite/PES matrix membrane

The composition of the casting solution of all prepared membranes is shown in Table 1.

Initially, a certain amount of NaX zeolite was dispersed in the DMF solvent and stirred at 200 rpm for 1 h at room temperature. Then, the PES polymer was added to the solution with continuous stirring at 300 rpm until the solution became homogeneous. The solution was left for a while to allow the complete release of air bubbles then the solution was cast on a clean glass plate using a casting knife. The glass plate was immediately immersed in a coagulation bath of water. The synthesized MMM's were stored in de-ionized water for 4 d for complete removal of the residual solvent. The MMM's were dried at room temperature for about 24 h. Fig. 1 summarizes the preparation procedure followed in this research study.

2.5. Characterization of zeolite and membranes

XRD analysis was performed for the synthesized NaX zeolite using the Philips instrument (X'pert diffractometer) to check the phase. The N_2 adsorption/desorption isotherms were performed to determine the surface area of the zeolite using the BET method. SEM images showing the morphology and EDAX analysis providing the chemical composition of both NaX zeolite and membranes were carried out using the Hitachi SU500 model device. FTIR test was conducted to detect the functional groups of NaX zeolite and the prepared membranes using the ALPHA, 3000IR microscope model device.

Contact angle measurement was performed by dropping deionized water carefully on the top of the membrane surface. This test reflects the wettability nature of the membrane. The average of three measurements at randomly chosen locations was taken for each sample to reduce the experimental error. The membrane porosity was determined through a gravimetric method reported by [31]. Briefly, the dried membranes were weighed and immersed in distilled water at room temperature for 24 h. After that, the membranes were wiped with tissue papers to remove the excess water from the surface and then weighed again [32]. The porosity of the membrane was calculated using Eq. (1) [33]:

$$\varepsilon = \frac{\left(w_1 - w_2\right)}{\left(A \times T \times \rho\right)} \times 100 \quad (1)$$

where w_1 and w_2 are the mass of the wet membrane and dry membrane (g), respectively. A is the area of a membrane (cm^2), T is the thickness of a membrane (cm), and ρ is the density of the water (g/cm^3). The membrane thickness was measured using a modern scan microscope device (model Waco/VSM). Finally, AFM was used to determine the pore size and pore size distribution of the membranes. AFM

Table 1
The composition of the polymeric solutions made to prepare flat sheet MMM's (PES of 20%wt.)

Membrane sample code	Zeolite (wt.%)	DMF (wt.%)
M0	0	80
M1	0.3	79.7
M2	0.6	79.4
M3	0.9	79.1
M4	1.2	78.8

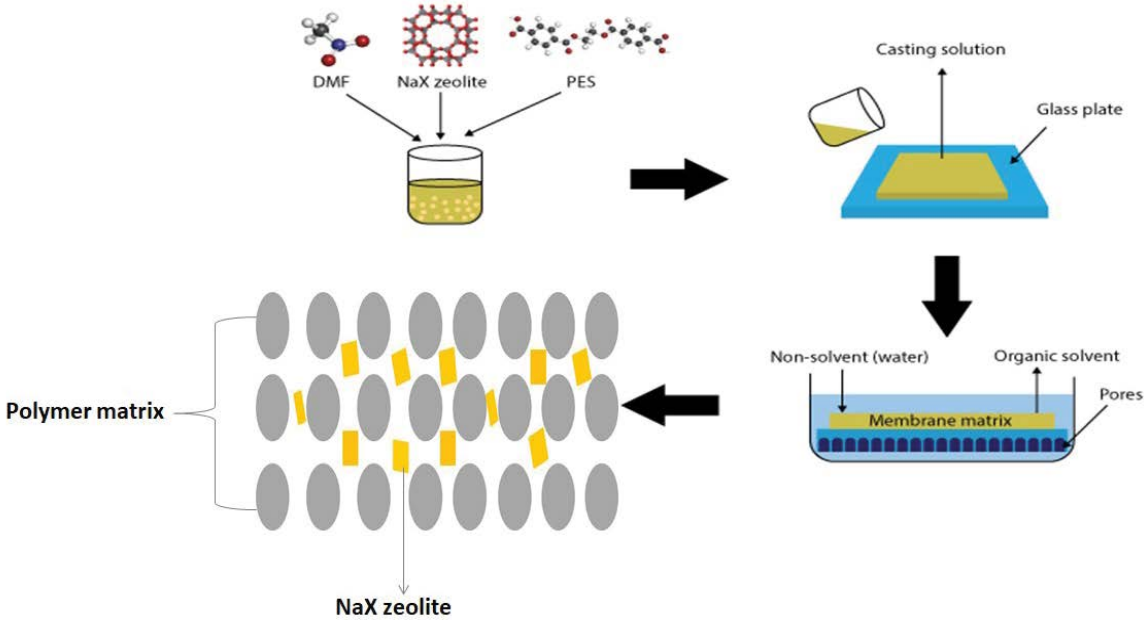

Fig. 1. Schematic of the preparation of zeolite/PES matrix membranes via phase inversion method.

was carried out using the fast scan microscope (Angstrom Advanced Inc., (USA), model AA3000). The pH drift method was used to measure the point of zero charge (pH_{zcp}) of the membrane [34] in which, pieces of membrane film were soaked in the NaCl solution with pH ranging from 3 to 12. A piece of membrane film (2 × 2 cm^2) was added to 20 mL of 0.1 M NaCl solution. Then, the final pH of the solutions was measured after 24 h. Then, the difference between the final pH and initial pH was plotted against the initial pH to obtain the value of pH_{zcp}.

2.6. Removal of metal ions

The performance of the prepared MMM's was measured by a cross-flow system in which the feed stream flowed tangentially to the membrane surface as shown in Fig. 2. The effective area of each used flat sheet membrane was 16.24 cm^2. The filtration experiments were conducted at 25°C and TMP of 1.6 bar. Pure water permeability was obtained by measuring the permeate volume of distilled water passing through a membrane after 90 min. The membrane performance was also tested using an aqueous solution with a feed concentration of 50 ppm of Pb(II) ions. The permeate flux, J, (L/m^2 h or LMH) is calculated using Eq. (2) and the metal ions rejection (%R) is calculated using Eq. (3) [35,36].

$$J = \frac{v}{A \times t} \tag{2}$$

$$\%R = \left(1 - \frac{C_P}{C_F}\right) \times 10 \tag{3}$$

where v is the permeate volume (L), A is the effective membrane area (m^2), t is the operation time (min), C_P is the metal ions concentration in the permeate solution, and C_F is the metal ions concentration in the feed solution. The values of C_P and C_F were obtained from measuring the metal ions concentration in permeate and feed solutions using the atomic absorption spectrometry model Perkin Elmer 5000.

3. Results and discussion

3.1. Characterization of NaX zeolite

Fig. 3 shows the XRD pattern of the prepared NaX zeolites which displays identical peaks to those obtained by [29,30]. The main peaks appeared in the XRD pattern at 2θ values of 5°, 10°, and 24° justify obtaining pure phase NaX zeolite. Also, the flat background of the pattern confirms obtaining a full crystalline product.

The Si/Al ratio of the synthesized NaX zeolite obtained by EDAX analysis was 1.2 and the sodium content was 4.43%wt. The morphology of the synthesized NaX zeolite shown by SEM images present in Fig. 4b confirms obtaining a fully crystallized product. The average crystal size of NaX was determined using 90 pulse particle sizing software device and found to be 117.2 nm.

Fig. 5 shows the FTIR results of NaX zeolite. A peak that appeared at the range of 677–954 cm^{-1} corresponds to bending TO_4, a peak at 3,556 cm^{-1} is assigned to the existence of the OH group attached to Na^+. A peak at 1,026 cm^{-1} is attributed to the vibration of Si–O–Al and Si–O–Si tetrahedron. Fig. 6 shows the N_2 adsorption–desorption isotherm of type I isotherms which indicates obtaining a microporous structure of NaX zeolite. The surface area and pore volume of the prepared NaX zeolite was 328.3297 m^2/g and 0.202460 cm^3/g, respectively, which are smaller than those obtained by [37] which can be attributed to using different silica source.

3.2. Characterization of membranes

3.2.1. Membrane morphology

The morphology of the top surface and cross-section of the prepared MMM's is shown in Fig. 7. Fig. 7 (A0-A4) shows the membrane top surface where there

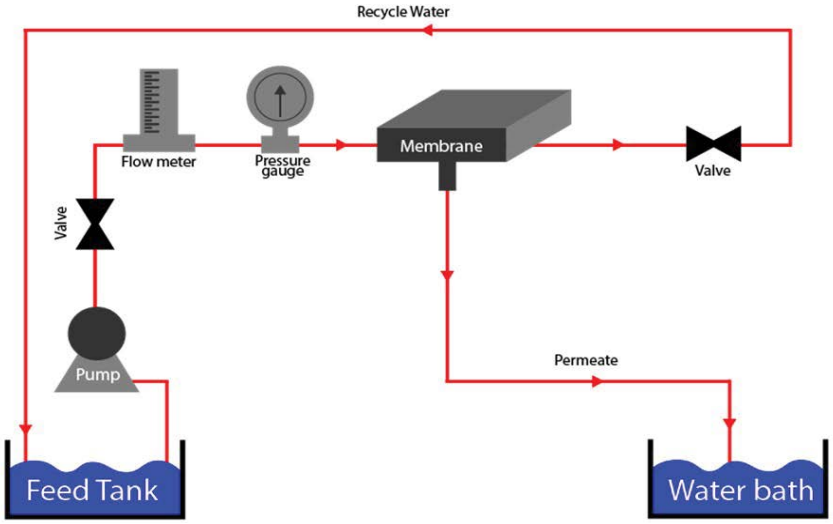

Fig. 2. Schematic diagram of the filter equipment.

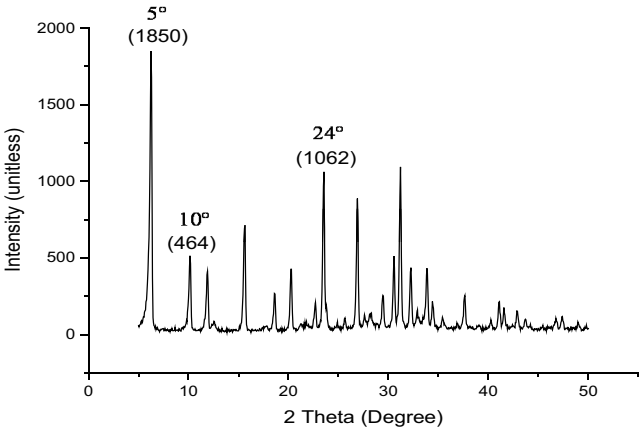

Fig. 3. The XRD patterns of the synthesized NaX zeolite.

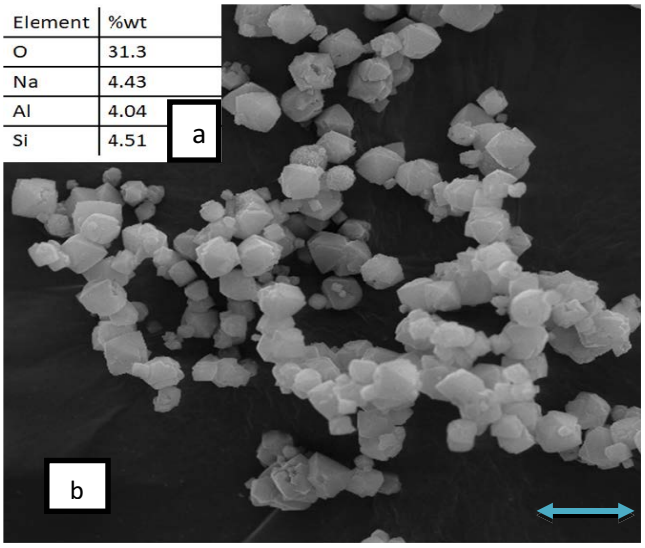

Fig. 4. (a) Elements analysis of NaX zeolite by EDAX, (b) SEM image of the prepared NaX zeolite (hydrothermal crystallization at 100°C for 6 h). (Scale bar = 10 μm).

are crystals on the top of the PES for membranes (M1 to M4). The layer containing zeolite crystals acts as a separation layer (upper layer), while the PES support layer acts as a support layer (bottom layer). SEM images in Fig. 7 (B0–B4) shows the formation of large finger-like pores across the entire sublayer with a thin upper layer. Whilst, further increase in the zeolite concentration above 1% for M5 led to formation of dissimilar pores and a thinner upper layer.

The surface roughness of the prepared membranes due to adding nanoparticles of zeolite was studied through the AFM analysis and the results are shown in Fig. 7 (C0–C4). It can be observed that NaX zeolite affects the roughness of the membrane as adding of zeolite particles to the PES membrane made the membrane rougher. The membrane roughness increased with an increase in the concentration of the NaX zeolite particles added to the casting solution. The roughness was 3.43 nm for M0, but it increased gradually to 4.11, 6.62, 6.73, and 7.04 nm for M1, M2, M3, and M4 respectively.

3.2.2. EDAX and FTIR spectra

The elemental composition of M1 was obtained from EDAX results shown in Fig. 8a. Al, Si, Na, and O appeared due to the presence of NaX zeolite. Also, appearing of C, S, and O is attributed to the polymer PES forming the MMM's.

The FTIR spectra displayed in Fig. 8b show the functional groups of M0, M1, M2, M3, and M4 in comparison with that of M0. FTIR spectra of M0 shows several peaks at 1,577; 1,481; 1,319 and 1,010 cm^{-1} corresponding to the stretching vibrations of C=C, C–H, S=O, and C–O–C in PES. The same of these peaks appeared in the spectra of M1, M2, M3, and M4. The presence of zeolite within the PES matrix was indicated by the peak at 3,750 cm^{-1} appearing in M1, M2, M3, and M4, which is a very small peak due to using small content of NaX zeolite. While the peaks at 710 and 1,009 cm^{-1} refer to the symmetric and asymmetric tetrahedron (TO_4, where T=Al, Si) of zeolite respectively. Also, these peaks appeared in the spectra of M1, M2, M3, and M4.

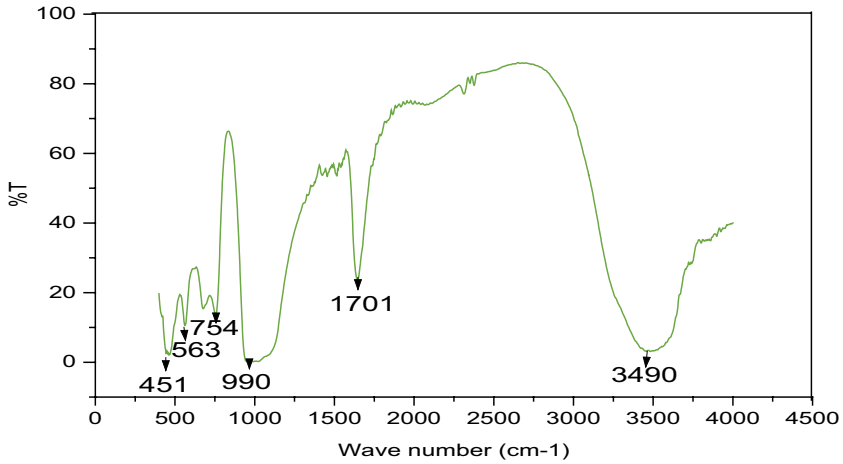

Fig. 5. FTIR spectra of NaX zeolite.

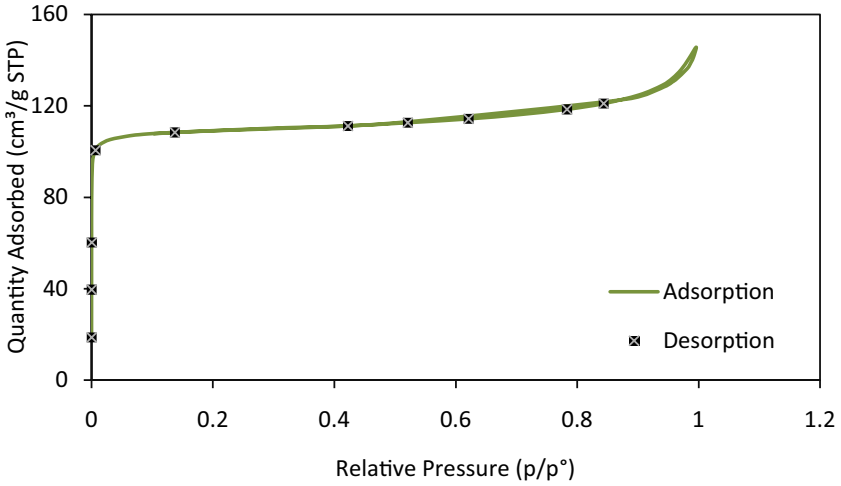

Fig. 6. N_2 adsorption/desorption isotherm.

3.2.3. Contact angle

The hydrophilicity of all prepared membranes was evaluated by measuring the contact angle and the results are shown in Fig. 9 and Table 2. It was observed that the contact angle reduced with adding of NaX zeolite. The hydrophilicity of all MMM's enhanced due to the hydrophilic nature of the used additive. There is a relative increase in the contact angle for membranes M3 and M4 due to the zeolite loading being above 0.6%wt. This can be attributed to the aggregation of NaX zeolite and the reduction in the effective surface of the particles, which in turn led to an uneven distribution of NaX zeolite particles inside the matrix membrane.

3.2.4. Thickness and porosity

The thickness of the prepared MMM's at various NaX zeolite percentages is shown in Table 2. It can be observed that the thickness of the membrane increased with increasing the concentration of NaX zeolite within MMM (i.e., increasing the solid particles in the casting solution resulted in increasing the membrane thickness) [38]. The porosity of the prepared membranes decreased with the increase in the concentration of zeolite added to the casting solution. The porosity of pure membrane M0 was 62.7% but it decreased to 59.2%, 54.5%, 45.5%, and 42% for M1, M2, M3, and M4, respectively (Table 2). Adding NaX zeolite nanoparticles to the casting solution changed the properties of the solution, resulting in a fast exchange between the solvent and non-solvent during phase inversion. Consequently, the porosity of the matrix membrane was higher than those of the pure PES membrane. On the other hand, the viscosity of the casting solution has a significant impact on the morphology and structure of the prepared membranes. Adding NaX zeolite nanoparticles to the casting solution led to increasing in the solution viscosity causing a lower exchange rate between the solvent and nonsolvent during the phase inversion and delayed de-mixing. As a result, the porosity of the membrane decreased. These results are in agreement with [33].

3.3. Separation performance of membranes

3.3.1. Effect of zeolite percentage

The effect of NaX zeolite loading on the performance of the prepared PES membrane and MMM's represented by the water permeate and rejection of Pb(II) ions were examined using a feed solution containing 50 ppm of Pb(II) ions at a feed temperature of 25°C and TMP of 1.6 bar. The results are shown in Fig. 10. The permeability increased with adding NaX zeolite up to 0.6%wt. and then declined with further adding of NaX zeolite. Fig. 10a shows that the permeate flux of M0 was 5.54 LMH; and it was 289.4, 487.68, 88.05, and 123.15 LMH for M1, M2, M3, and M4, respectively. This behavior can be explained as that adding NaX zeolite improved the hydrophilicity of the prepared MMM's. Fig. 10b shows that the rejection of Pb(II) ions was 29% for M0 while it was 46% and 45.2% for M1 and M2, respectively. The highest rejection of Pb(II) ions was obtained by M3 where it was 97%, and then it gradually reduced to 57.4% by M4. The high effectiveness of the M3 was perhaps attributed to the uniform distribution of NaX zeolite enhancing the permeability of the membrane and providing active sites for capturing Pb(II) ions.

Table 3 shows a comparison between the prepared membrane M3 with the other reported in the literature for the removal of Pb(II) ions. This comparison was made with the recently published data found in the literature based on the permeate flux and %Rejection of the MMM's. It can be noticed that the performance of M3 prepared in the current work showed excellent Pb(II) removal efficiency and acceptable permeate flux in comparison with most of the MMM's in the literature.

3.3.2. Effect of pH solution

Fig. 11a shows the effects of the feed pH on the permeate flux and the Pb(II) ions rejection using M3 at feed temperature of 25°C, TMP of 1.6 bar, and feed solution of Pb(II) ions of 50 ppm. It can be observed that the permeate flux was 88, 59, and 14 LMH when feed pH was 6, 4 and 2, respectively.

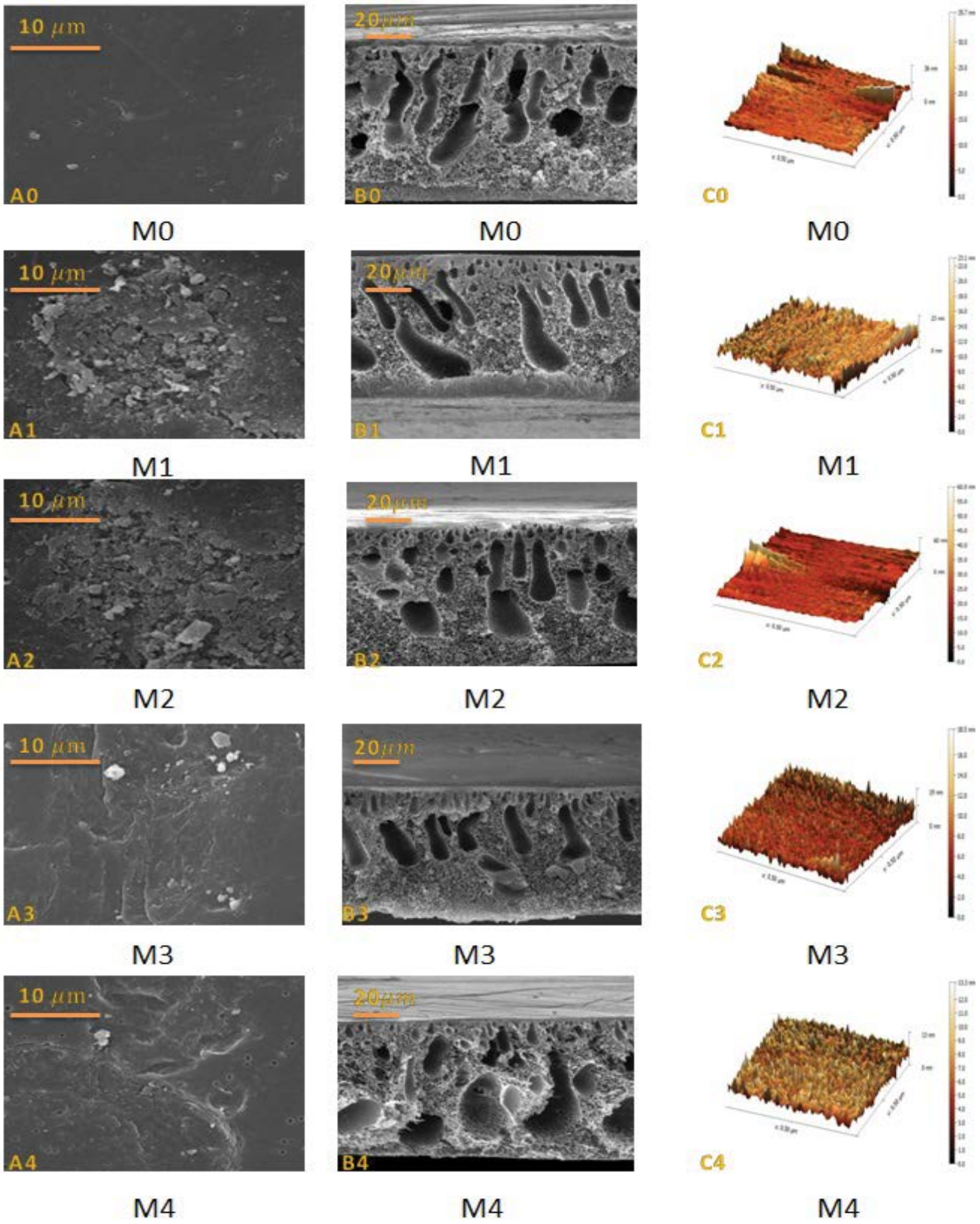

Fig. 7. (A0–A4) SEM images for the top surface, (B0–B4) SEM images for the cross section, and (C0–C4) AFM for the top surface of the prepared membranes.

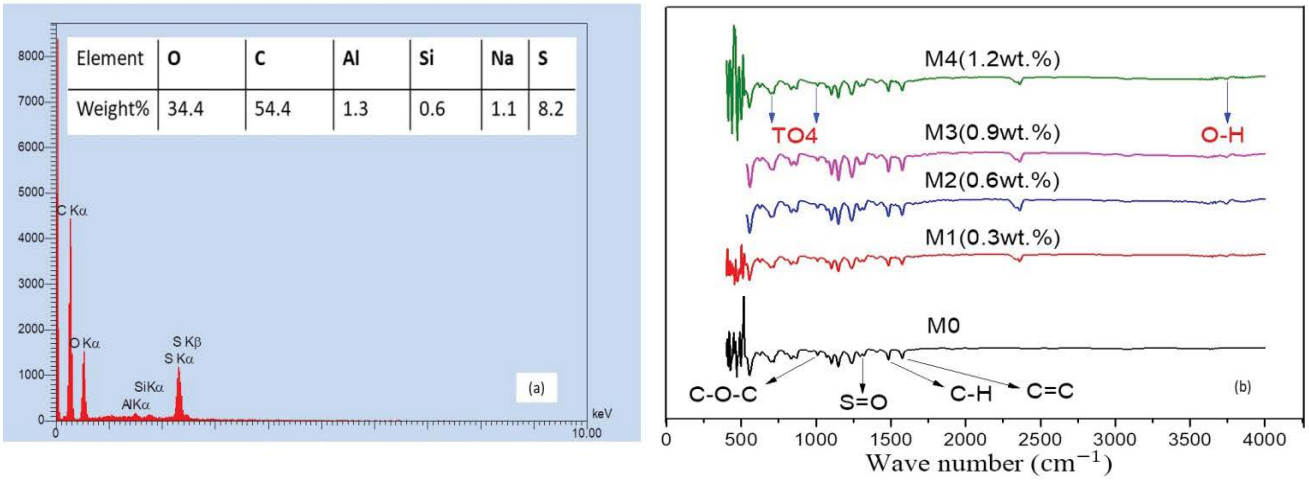

Fig. 8. (a) EDAX of (M1) membrane and (b) FTIR spectra of all prepared membranes.

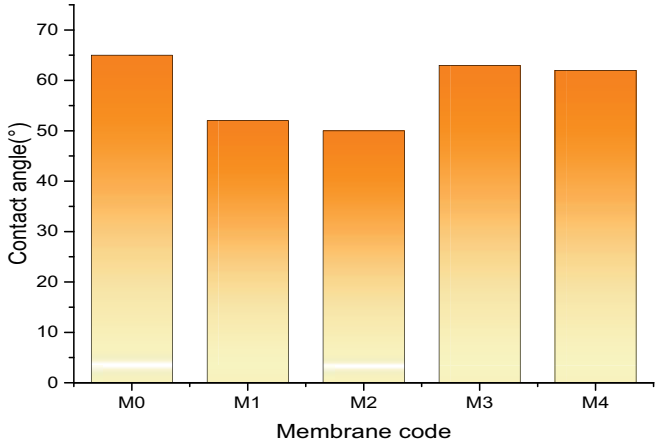

Fig. 9. The contact angle of the prepared membranes.

Table 2
Characterization of the thickness and porosity of the membranes

Membrane	Concentration of NaX zeolite within a membrane (wt.%)	Contact angle (°)	Thickness (μm)	Porosity (%)
M0	0	65	157.4	62.7
M1	0.3	52	187.9	59.2
M2	0.6	50	198.1	54.5
M3	0.9	63	203.2	45.5
M4	1.2	62	279.4	42

This can be interpreted as the decrease in pH due to adding of hydrochloric acid to the solution led to changes in the viscosity of the solution and an increase in the osmotic pressure which reduced the flux. The highest flux of 88 LMH was achieved at a pH of 6. This behavior is in agreement with [48]. Fig. 11b shows increasing the %rejection of Pb(II) ions with rising the pH of the solution from 2 to 6 to achieve the highest rejection of 97%, then it reduced to about 88% at pH of 7.

This behavior of M3 at different pH media can be explained by measuring the pH_{zcp} (Fig. 12). The results present in this figure shows that the pH_{zcp} was just below 7.1. Therefore at pH between 3 and 7.1, the PES membrane has a positive-charged surface and this positive charge reached the maximum at pH equals 6. This high positive charge induced the repulsion between the membrane surface and the metal cations and thus, high rejection was

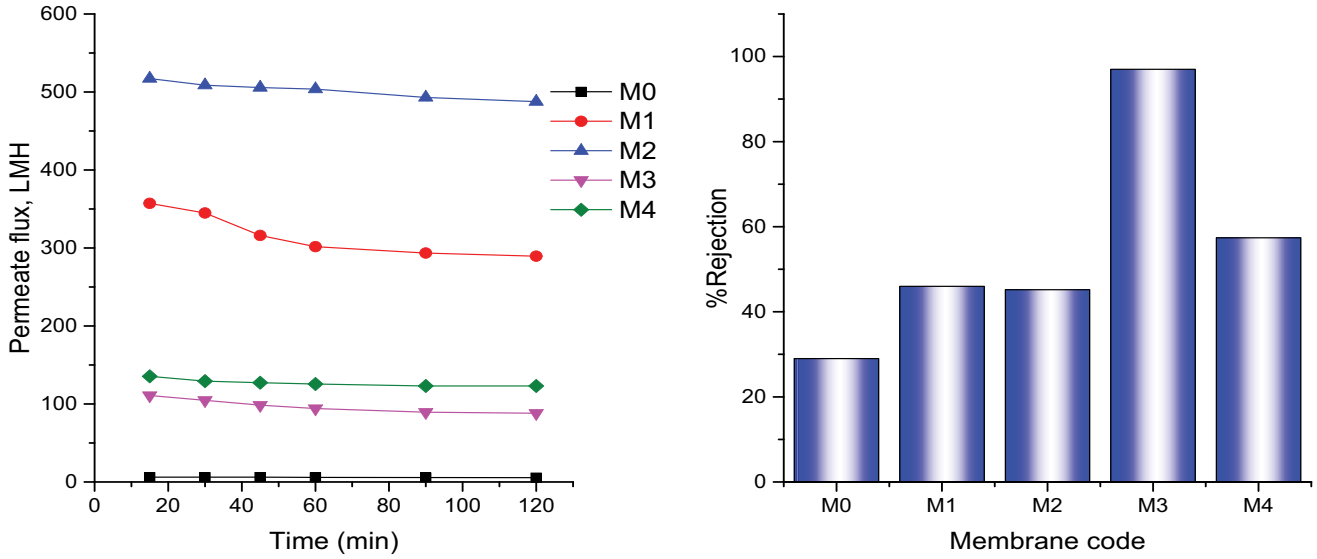

Fig. 10. Effect of zeolite content in the prepared membranes on (a) the permeate flux, (b) %Rejection of Pb(II) ions at Pb(II) ions concentration of 50 ppm, pH of 6, and TMP of 1.6 bar.

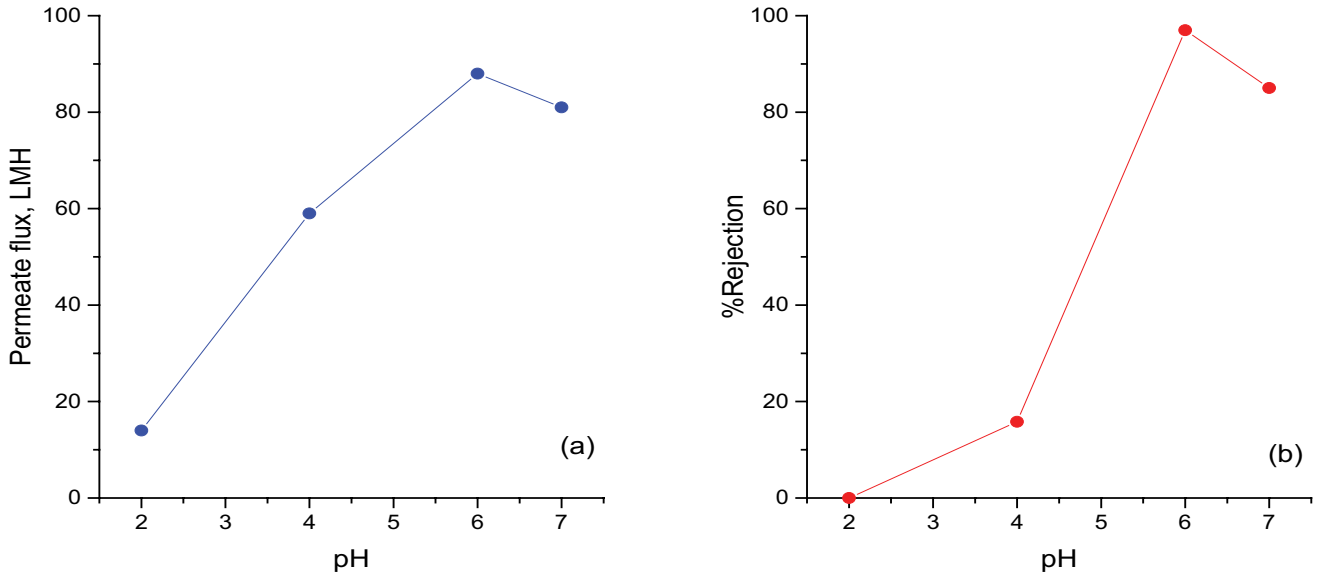

Fig. 11. Effect of feed pH value on (a) permeate flux and (b) %Rejection of Pb(II) ions for M3 at Pb(II) ions concentration of 50 ppm, and TMP of 1.6 bar.

obtained when Pb(II) ions present in a solution with a pH of 6. However, Fig. 12 shows that the membrane surface tends to be negative at a pH of 2 which explains the low rejection of Pb(II) ions by M3. Also, the membrane surface tends to be less positive-charged during rising the pH from 6 to 7, negative-charged at pH above 7.1. This elucidates the reduced %Rejection of Pb(II) ions (about 85%) by M3 during treating a solution of Pb(II) ions at a pH of 7. It was observed that the metal solution color changed to cloudy at a pH = 7 which can be attributed to precipitation of the metal hydroxide which participated in the removal of metal ions. The results of this study agreed with those obtained by [49] which involve investigating the removal of Pb(II) ions and Cd(II) ions from a single salt using a PES hollow fiber membrane at different pH. Fig. 11b shows decreasing the rejection of Pb(II) ions with decreasing the pH of the solution from 6 to 2 which is attributed to the above-mentioned reasons.

3.3.3. *Effect of initial Pb(II) ions concentrations*

Fig. 13a illustrates the effect of changing the Pb(II) ions concentrations from 50 to 200 ppm on the permeate flux of M3 membrane at a feed temperature of 25°C, pH of 6, and TMP of 1.6 bar. The results show that the permeate flux decreased from 88 to 74.9 LMH as the initial Pb(II)

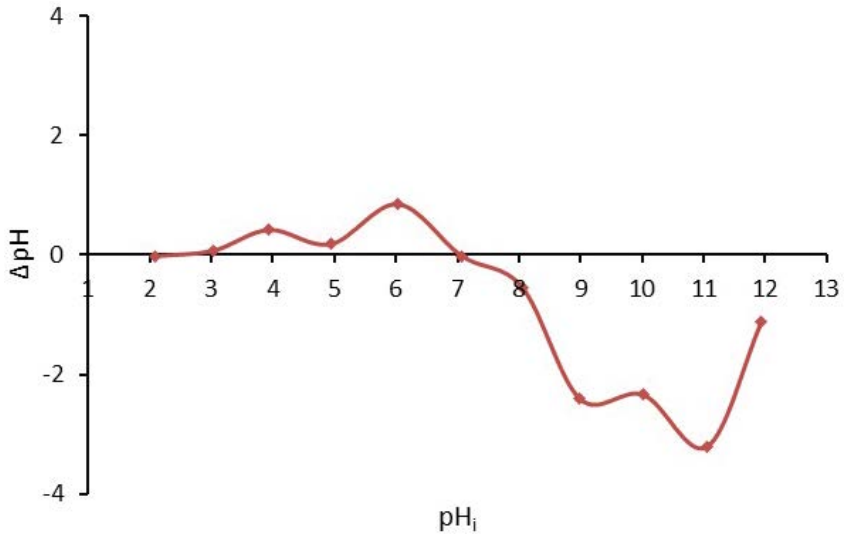

Fig. 12. Zero charge point of M3.

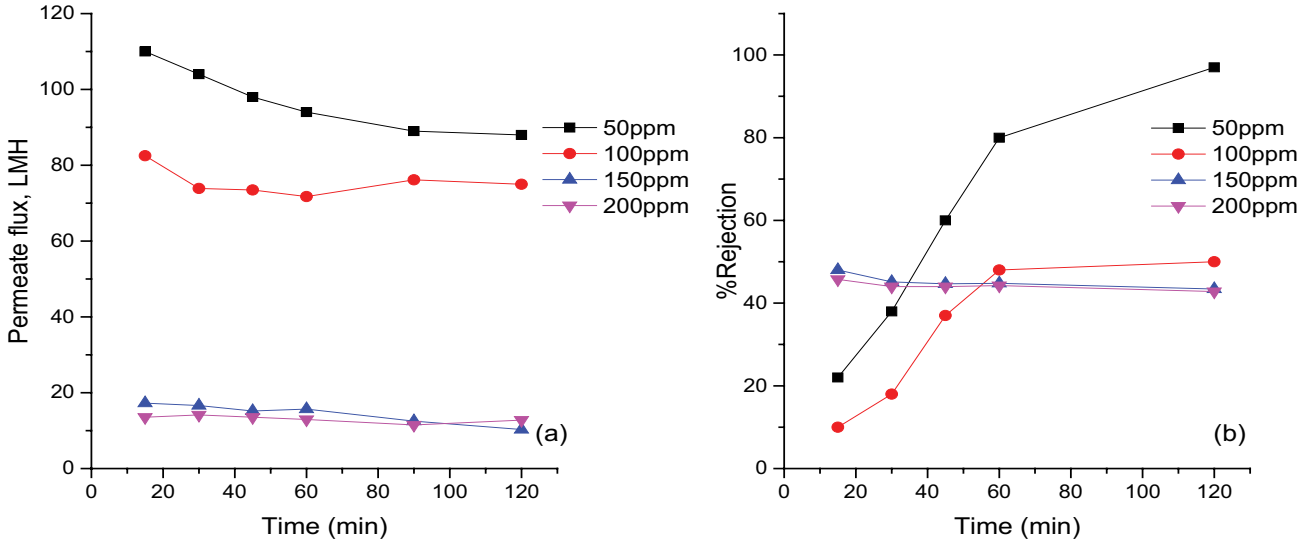

Fig. 13. Effect of feed concentration of Pb(II) ions on (a) the permeate flux and (b) %Rejection of Pb(II) ions for M3 at pH of 6, and TMP of 1.6 bar.

ions concentration increased from 50 to 100 ppm. Further decline in the permeate flux occurred when the initial Pb(II) ions concentration increased to 150 and 200 ppm. These results can be explained as increasing the retention of Pb(II) ions on the membrane surface can decrease the effective pore size. Moreover, increasing the concentration of Pb(II) ions would generate a cake layer on the membrane surface and reduce the permeability of the prepared membrane. These results well agreed with those obtained by [31,50]. The effect of changing the initial Pb(II) ions concentration on the rejection by M3 is shown in Fig. 13b. The rejection of Pb(II) ions decreased as the Pb(II) ions concentration increased. Where the rejection of Pb(II) ions reduced as 50%, 43.4%, and 42.8% at a feed concentration of 100, 150, and 200 ppm, respectively.

3.3.4. Effect of feed temperature

Fig. 14 shows the permeate flux and rejection of Pb(II) ions using M3 as a function of temperature for the feed solution containing 50 ppm of Pb(II) ions and at TMP of 1.6 bar. The results show that the permeate flux increased for high feed solution temperature. The permeate flux increased as 88, 142, and 283 LMH when the feed solution temperature was 25°C, 36°C, and 46°C, respectively. Whilst, the rejection of Pb(II) ions decreased as feed temperature increased. The rejection of Pb(II) ions was 50.8% and 49.6% when the temperature of the feed solution was 36°C and 46°C, respectively. These results could perhaps be because of changing the surface structure of the membrane in terms of the average pore size with increasing the feed temperature which leads to reducing

Table 3
Comparison between the performances of membranes prepared in this study with various MMM's in the literature in the terms of total pure water flux, and removal efficiency

Polymer	Fillers	Permeate flux (LMH)	Initial conc. (ppm)	Temperature (°C)	pH	Time (min)	Pb(II) rejection (%)	References
PSF (15 wt.%)	NaX zeolite (10 wt.%)	57	100	NA	NA	60	91%	[39]
PES (20 wt.%)	ZIF-67/cGO nanohybrid (0.5 wt.%)	346.4 ± 11.2	10	NA	Natural pH	NA	97.8%	[40]
PSF (18 wt.%)	EDTA-bentonite particle (2 wt.%)	26	50	NA	5	60	98%	[41]
PPSU (18 g)	CNT (0.3 wt.%)	>185	500	25°C	6 ± 0.2	60	<98%	[42]
PSF (10.17 wt.%)	HFO NPs (15.25 wt.%)	942.1	0.1	Room Temp.	6.5–7	NA	96%	[43]
PSF (20 wt.%)	GO (0.2)	50–45	50	NA	6.7	60	~96%	[44]
CA (1.5 g)	VTES-GO (1–5 wt.%)	8.6	20	NA	9	900	97.6%	[45]
PEI (18 g)	MHNTs (0.54 g)	<250	1000	29°C	6 ± 0.5	80	79%	[46]
PVDF (12 wt.%)	SnNPs (0.25 wt.%)	28.9 ± 2.1	7.5 ± 0.2	NA	7	15	93.9%	[47]
PES (20 wt.%)	NaX zeolite (0.9 wt.%)	88.05	50	Room Temp.	6	120	97%	Current study

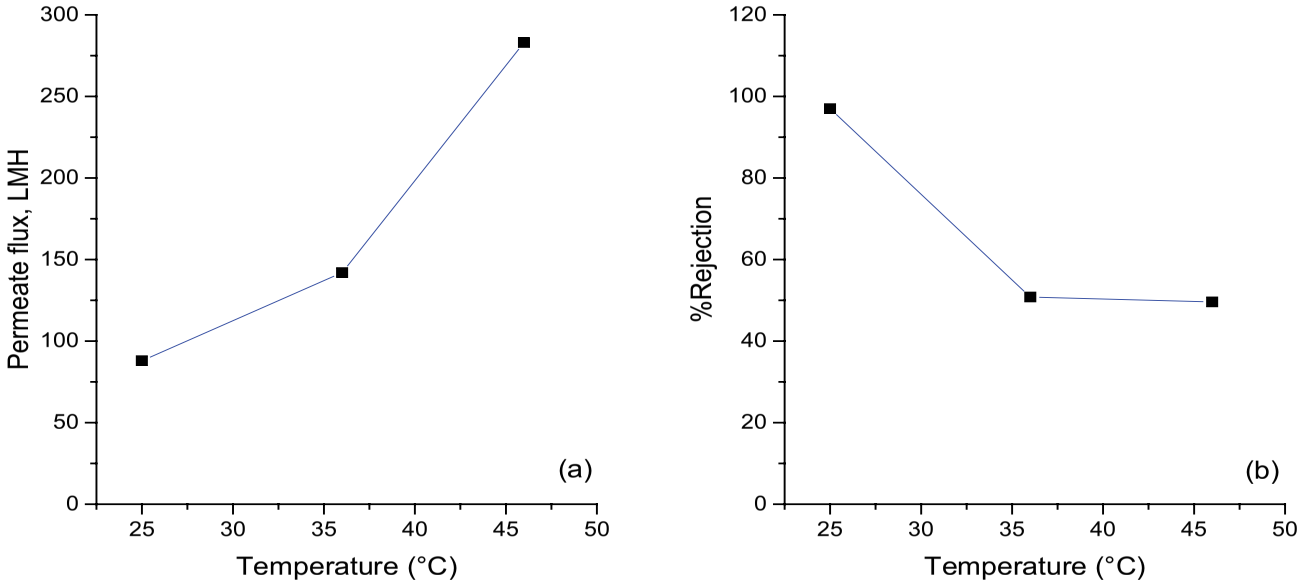

Fig. 14. Effect of feed temperature on (a) permeate flux and (b) %Rejection of Pb(II) ions for M3 at Pb(II) concentration of 50 ppm, pH of 6, and TMP of 1.6 bar.

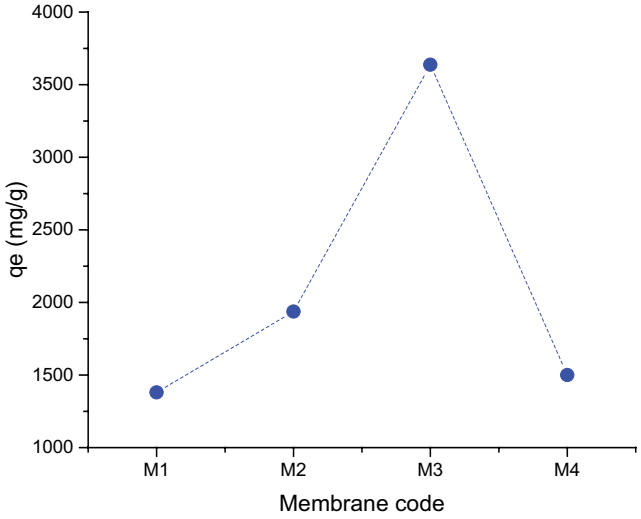

Fig. 15. The adsorption of Pb(II) ions by the prepared membranes at pH of 6, and initial concentration of Pb(II) of 50 ppm.

the viscosity of the feed solution, increasing the permeability and the ions diffusion coefficient. These results agreed with those obtained by [51,52].

3.4. Studying the adsorption capacity of the zeolite embedded in PES membranes

The adsorption capacity of the zeolite embedded in PES membranes used for Pb(II) ions removal was examined at equilibrium time, feed temperature of 25°C, TMP of 1.6 bar, and Pb(II) ions concentration of 50 ppm. The adsorption capacity results were calculated using Eq. (4) [37].

$$q_e = \left(C_o - C_e\right) \times \frac{v}{w} \tag{4}$$

where q_e is the adsorption capacity of zeolite content at equilibrium (mg/g), V is the solution volume (L), W is the weight of dry membrane (g), C_o and C_e are the concentrations of lead(II) ions at t = 0 (min) and t = equilibrium time (min), respectively.

Fig. 15 shows that M3 has a higher adsorption capacity for Pb(II) ions than other membranes. The adsorption capacity of the zeolite in M3 membrane for Pb(II) ions was 3,637.5 mg/g. As early mentioned, the high effectiveness of the membrane M3 was perhaps attributed to the uniform distribution of NaX zeolite enhancing the permeability of the membrane and providing active sites for capturing Pb(II) ions (Fig. 16). Moreover, the negative charge density produced by NaX zeolite provides stronger electrostatic attraction between the membrane surface and Pb(II) ions and partly contributes to the removal rate [24].

4. Conclusions

In conclusion, NaX zeolite powder was successfully synthesized by the hydrothermal method. NaX zeolite was incorporated with different percentages in the PES membrane to enhance the performance of the ultrafiltration separation system for Pb(II) ions in the aqueous solution. The flat sheet MMM zeolite/PES was prepared by the phase inversion technique. The membrane became denser and the pore volume reduced with increasing the zeolite loading just above 0.6 wt%. Water permeation increased after adding NaX zeolite to the casting solution for all prepared MMM's due to the hydrophilic property of NaX zeolite. The highest rejection of Pb(II) ions obtained was 97% at feed temperature of 25°C, TMP of 1.6 bar, and initial Pb(II) concentration of 50 ppm using a membrane containing 0.9%wt. zeolite.

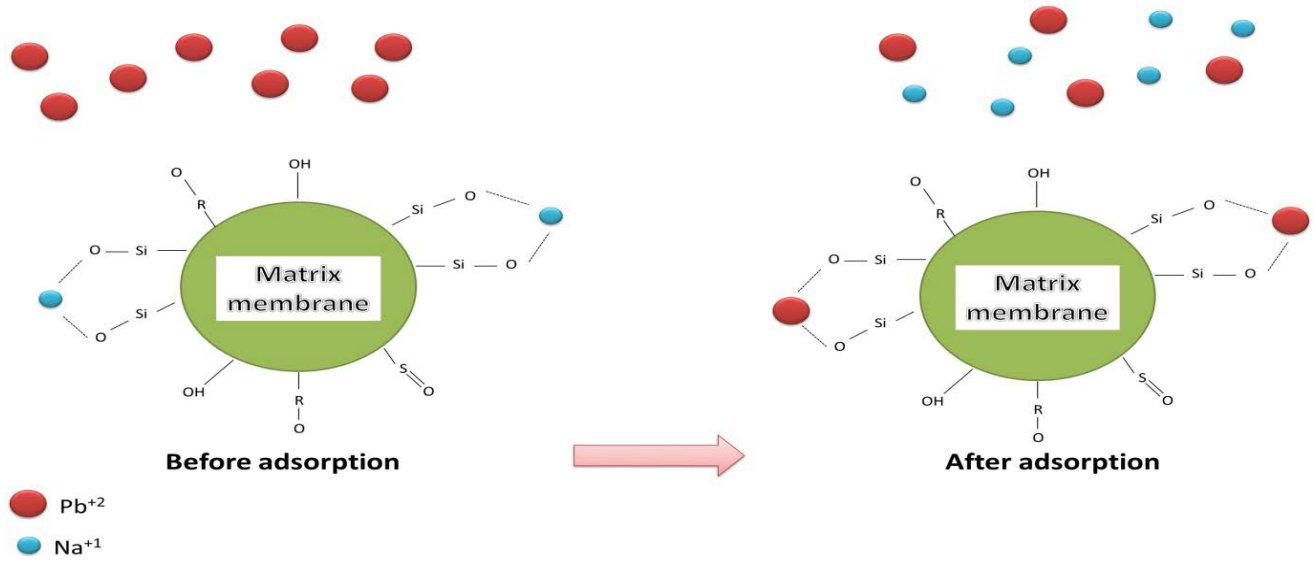

Fig. 16. Schematic of mechanism for adsorption Pb(II) ions onto membrane surface.

References

[1] A.S. Mohammed, A. Kapri, R. Goel, Biomanagement of Metal-Contaminated Soils, Springer, Dordrecht, 2011, pp. 1–28.
[2] S. Kocaoba, Adsorption of Cd(II), Cr(III) and Mn(II) on natural sepiolite, Desalination, 244 (2009) 24–30.
[3] S.M. Al-Jubouri, H.A. Sabbar, H.A. Lafta, B.I. Waisi, Effect of synthesis parameters on the formation 4A zeolite crystals: characterization analysis and heavy metals uptake performance study for water treatment, Desal. Water Treat., 165 (2019) 290–300.
[4] R.H. Salman, H.A. Hassan, K.M. Abed, A.F. Al-Alawy, D.A. Tuama, K.M. Hussein, H.A. Jabir, Removal of chromium ions from a real wastewater of leather industry using electrocoagulation and reverse osmosis processes, AIP Conf. Proc., 2213 (2020) 020186, doi: 10.1063/5.0000201.
[5] R. Laus, T.G. Costa, B. Szpoganicz, V.T. Fávere, Adsorption and desorption of Cu(II), Cd(II) and Pb(II) ions using chitosan crosslinked with epichlorohydrin-triphosphate as the adsorbent, J. Hazard. Mater., 183 (2010) 233–241.
[6] A. Çelekli, H. Bozkurt, Bio-sorption of cadmium and nickel ions using *Spirulina platensis*: kinetic and equilibrium studies, Desalination, 275 (2011) 141–147.
[7] M. Naushad, A. Mittal, M. Rathore, V. Gupta, Ion-exchange kinetic studies for Cd(II), Co(II), Cu(II), and Pb(II) metal ions over a composite cation exchanger, Desal. Water Treat., 54 (2015) 2883–2890.
[8] A. Shahat, M.R. Awual, M.A. Khaleque, M.Z. Alam, M. Naushad, A.S. Chowdhury, Large-pore diameter nano-adsorbent and its application for rapid lead(II) detection and removal from aqueous media, Chem. Eng. J., 273 (2015) 286–295.
[9] P.N. Obasi, B.B. Akudinobi, Potential health risk and levels of heavy metals in water resources of lead–zinc mining communities of Abakaliki, southeast Nigeria, Appl. Water Sci., 10 (2020) 1–23.
[10] A. Almasi, M. Omidi, M. Khodadadian, R. Khamutian, M.B. Gholivand, Lead(II) and cadmium(II) removal from aqueous solution using processed Walnut shell: kinetic and equilibrium study, Toxicol. Environ. Chem., 94 (2012) 660–671.
[11] A.A. Faisal, S.F. Al-Wakel, H.A. Assi, L.A. Naji, M. Naushad, Waterworks sludge-filter sand permeable reactive barrier for removal of toxic lead ions from contaminated groundwater, J. Water Process. Eng., 33 (2020) 101112, doi: 10.1016/j.jwpe.2019.101112.
[12] W.W. Ngah, S. Fatinathan, Adsorption characterization of Pb(II) and Cu(II) ions onto chitosan-tripolyphosphate beads: kinetic, equilibrium and thermodynamic studies, J. Environ. Manage., 91 (2010) 958–969.
[13] Y. Tian, M. Wu, R. Liu, Y. Li, D. Wang, J. Tan, R. Wu, Y. Huang, Electrospun membrane of cellulose acetate for heavy metal ion adsorption in water treatment, Carbohydr. Polym., 83 (2011) 743–748.
[14] H.M. Rashid, A.A. Faisal, Removal of dissolved cadmium ions from contaminated wastewater using raw scrap zero-valent iron and zero valent aluminum as locally available and inexpensive sorbent wastes, Iraqi J. Chem. Pet. Eng., 19 (2018) 39–45.
[15] A. Abbas, A.M. Al-Amer, T. Laoui, M.J. Al-Marri, M.S. Nasser, M. Khraisheh, M.A. Atieh, Heavy metal removal from aqueous solution by advanced carbon nanotubes: critical review of adsorption applications, Sep. Purif. Technol., 157 (2016) 141–161.
[16] D.A. de Haro-Del Rio, S.M. Al-Jubouri, S.M. Holmes, Hierarchical porous structured zeolite composite for removal of ionic contaminants from waste streams, Chim. Oggi – Chem. Today, 35 (2017) 56–58.
[17] S.M. Al-Jubouri, S.I. Al-Batty, R. Ramsden, J. Tay, S.M. Holmes, Elucidation of the removal of trivalent and divalent heavy metal ions from aqueous solutions using hybrid-porous composite ion exchangers by nonlinear regression, Desal. Water Treat., 236 (2021) 171–181.
[18] L.B. Chaudhari, Z.V.P. Murthy, Separation of Cd and Ni from multicomponent aqueous solutions by nanofiltration and characterization of membrane using IT model, J. Hazard. Mater., 180 (2010) 309–315.
[19] J. Kheriji, D. Tabassi, B. Hamrouni, Removal of Cd(II) ions from aqueous solution and industrial effluent using reverse osmosis and nanofiltration membranes, Water Sci. Technol., 72 (2015) 1206–1216.
[20] M.I.A. Wahab, H.I. Saleh, A.F. Al-Alawy, Performance of manipulated direct osmosis in water desalination process, Int. J. Sci. Technol., 4 (2015) 458–468.
[21] E. Saljoughi, S.M. Mousavi, Preparation and characterization of novel polysulfone nanofiltration membranes for removal of cadmium from contaminated water, Sep. Purif. Technol., 90 (2012) 22–30.
[22] N. Abdullah, N. Yusof, W.J. Lau, J. Jaafar, A.F. Ismail, Recent trends of heavy metal removal from water/wastewater by membrane technologies, J. Ind. Eng. Chem., 76 (2019) 17–38.
[23] D.M. Warsinger, S. Chakraborty, E.W. Tow, M.H. Plumlee, C. Bellona, S. Loutatidou, L. Karimi, A.M. Mikelonis, A. Achilli, A. Ghassemi, L.P. Padhye, A review of polymeric membranes and processes for potable water reuse, Prog. Polym. Sci., 81 (2018) 209–237.
[24] S. Shahrin, W.J. Lau, P.S. Goh, A.F. Ismail, J. Jaafar, Adsorptive mixed matrix membrane incorporating graphene oxide-manganese ferrite (GMF) hybrid nanomaterial for efficient As(V) ions removal, Compos. B. Eng., 175 (2019) 107150, doi: 10.1016/j.compositesb.2019.107150.
[25] S. Xiao, X. Huo, S. Fan, K. Zhao, S. Yu, X. Tan, Design and synthesis of Al-MOF/PPSU mixed matrix membrane with pollution resistance, Chin. J. Chem. Eng., 29 (2021) 110–120.
[26] S.M. Al-Jubouri, B.I. Waisi, S.M. Holmes, Rietveld texture refinement analysis of linde type a zeolite from X-ray diffraction data, J. Eng. Sci. Technol., 13 (2018) 4066–4077.
[27] S.M. Al-Jubouri, Synthesis of hierarchically porous ZSM-5 zeolite by self-assembly induced by aging in the absence of seeding-assistance, Microporous Mesoporous Mater., 303 (2020) 110296, doi: 10.1016/j.micromeso.2020.110296.
[28] S.M. Al-Jubouri, S.I. Al-Batty, S.M. Holmes, Using the ash of common water reeds as a silica source for producing high purity ZSM-5 zeolite microspheres, Microporous Mesoporous Mater., 316 (2021) 110953, doi: 10.1016/j.micromeso.2021.110953.
[29] S.M. Al-Jubouri, D.A. de Haro-Del Rio, A. Alfutimie, N.A. Curry, S.M. Holmes, Understanding the seeding mechanism of hierarchically porous zeolite/carbon composites, Microporous Mesoporous Mater., 268 (2018) 109–116.
[30] S.M. Al-Jubouri, S.I. Al-Batty, S. Senthilnathan, N. Sihanonth, L. Sanglura, H. Shan, S.M. Holmes, Utilizing Faujasite-type zeolites prepared from waste aluminum foil for competitive ion-exchange to remove heavy metals from simulated wastewater, Desal. Water Treat., 231 (2021) 166–181.
[31] M. Abdullah, S. Al-Jubouri, Implementation of hierarchically porous zeolite-polymer membrane for chromium ions removal, IOP Conf. Ser.: Earth Environ. Sci, 779 (2021) 012099, doi: 10.1088/1755–1315/779/1/012099.
[32] A. Abdel-Karim, S. Leaper, M. Alberto, A. Vijayaraghavan, X. Fan, S.M. Holmes, E.R. Souaya, M.I. Badawy, P. Gorgojo, High flux and fouling resistant flat sheet polyethersulfone membranes incorporated with graphene oxide for ultrafiltration applications, Chem. Eng. J., 334 (2018) 789–799.
[33] V. Moghimifar, A.E. Livari, A. Raisi, A. Aroujalian, Enhancing the antifouling property of polyethersulfone ultrafiltration membranes using NaX zeolite and titanium oxide nanoparticles, RSC Adv., 5 (2015) 55964–55976.
[34] M. Bourassi, M. Kárászová, M. Pasichnyk, R. Zazpe, J. Hercíková, V. Fíla, J.M. Macak, J. Gaálová, Removal of Ibuprofen from water by different types membranes, Polymers, 13 (2021) 4082, doi: 10.3390/polym13234082.
[35] S.M. Abdullah, Oily water treatment using ceramic memberane, J. Eng., 2 (2011) 252–264.
[36] S.H. Ahmed, S.M. Al-Jubouri, N. Zouli, A.A. Mohammed, H.S. Majdi, I.K. Salih, M. Al-Shaeli, A. Al-Rahawi, Q.F. Alsalhy, A. Figoli, Performance evaluation of polyethersulfone membranes for competitive removal of Cd^{2+}, Co^{2+}, and Pb^{2+}

ions from simulated groundwater, Geofluids, 2021 (2021), doi: 10.1155/2021/6654477.
[37] S.M. Al-Jubouri, S.M. Holmes, Hierarchically porous zeolite X composites for manganese ion-exchange and solidification: equilibrium isotherms, kinetic and thermodynamic studies, Chem. Eng. J., 308 (2017) 476–491.
[38] F.H. Al-Ani, Q.F. Alsalhy, R.S. Raheem, K.T. Rashid, A. Figoli, Experimental investigation of the effect of implanting Tio_2-nps on PVC for long-term UF membrane performance to treat refinery wastewater, Membranes, 10 (2020) 77, doi: 10.3390/membranes10040077.
[39] Y. Yurekli, Removal of heavy metals in wastewater by using zeolite nano-particles impregnated polysulfone membranes, J. Hazard. Mater., 309 (2016) 53–64.
[40] A. Modi, J. Bellare, Zeolitic imidazolate framework-67/carboxylated graphene oxide nanosheets incorporated polyethersulfone hollow fiber membranes for removal of toxic heavy metals from contaminated water, Sep. Purif. Technol., 249 (2020) 117160, doi: 10.1016/j.seppur.2020.117160.
[41] M. Dutta, A. Jana, S. De, Insights to the transport of heavy metals from an industrial effluent through functionalized bentonite incorporated mixed matrix membrane: process modeling and analysis of the interplay of various parameters, Chem. Eng. J., 413 (2021) 127397, doi: 10.1016/j.cej.2020.127397.
[42] N. Chandrashekhar, A.M. Isloor, B. Lakshmi, H.M. Marwani, I. Khan, Polyphenylsulfone/multiwalled carbon nanotubes mixed ultrafiltration membranes: fabrication, characterization and removal of heavy metals Pb^{2+}, Hg^{2+}, and Cd^{2+} from aqueous solutions, Arabian J. Chem., (2019), doi: 10.1016/j.arabjc.2019.10.007.
[43] N. Abdullah, R.J. Gohari, N. Yusof, A.F. Ismail, J. Juhana, W.J. Lau, T. Matsuura, Polysulfone/hydrous ferric oxide ultrafiltration mixed matrix membrane: preparation, characterization and its adsorptive removal of lead(II) from aqueous solution, Chem. Eng. J., 289 (2016) 28–37.
[44] R. Mukherjee, P. Bhunia, S. De, Impact of graphene oxide on removal of heavy metals using mixed matrix membrane, Chem. Eng. J., 292 (2016) 284–297.
[45] H. Idress, S.Z.J. Zaidi, A. Sabir, M. Shafiq, R.U. Khan, C. Harito, S. Hassan, F.C. Walsh, Cellulose acetate based complexation-NF membranes for the removal of Pb(II) from waste water, Sci. Rep., 11 (2021) 1–14, doi: 10.1038/s41598-020-80384-0.
[46] R.S. Hebbar, A.M. Isloor, K. Ananda, A.F. Ismail, Fabrication of polydopamine functionalized halloysite nanotube/polyetherimide membranes for heavy metal removal, J. Mater. Chem., 4 (2016) 764–774.
[47] Y. Ibrahim, V. Naddeo, F. Banat, S.W. Hasan, Preparation of novel polyvinylidene fluoride (PVDF)-Tin(IV) oxide (SnO_2) ion exchange mixed matrix membranes for the removal of heavy metals from aqueous solutions, Sep. Purif. Technol., 250 (2020) 117250, doi: 10.1016/j.seppur.2020.117250.
[48] J. Tanninen, M. Mänttäri, M. Nyström, Nanofiltration of concentrated acidic copper sulphate solutions, Desalination, 189 (2006) 92–96.
[49] S. Hadi, A.A. Mohammed, S.M. Al-Jubouri, M.F. Abd, H.S. Majdi, Q.F. Alsalhy, K.T. Rashid, S.S. Ibrahim, I.K. Salih, A. Figoli, Experimental and theoretical analysis of lead Pb^{2+} and Cd^{2+} retention from a single salt using a hollow fiber PES membrane, Membranes, 10 (2020) 136, doi: 10.3390/membranes10070136.
[50] M.G. Torkabad, A.R. Keshtkar, S.J. Safdari, Comparison of polyethersulfone and polyamide nanofiltration membranes for uranium removal from aqueous solution, Prog. Nucl. Energy, 94 (2017) 93–100.
[51] F. Zhou, C. Wang, J. Wei, Separation of acetic acid from monosaccharides by NF and RO membranes: performance comparison, J. Membr. Sci., 429 (2013) 243–251.
[52] X. Sun, C. Wang, Y. Tong, W. Wang, J. Wei, A comparative study of microfiltration and ultrafiltration for algae harvesting, Algal Res., 2 (2013) 437–444.